

THERMAL BEHAVIOR OF IRON NANOPARTICLES SYNTHESIZED BY CHEMICAL VAPOR CONDENSATION

Oleg V. Tolochko^{1*}, Chul-Jin Choi², Albert G. Nasibulin³,

Katerina S. Vasilieva¹, D.-W. Lee², D. Kim²

¹ Material Science Faculty, State Polytechnic University, Saint Petersburg, 195251 Russian Federation

² Korean Institute of Machinery and Materials, 66, Sangnam-Dong, Changwon, Kyungnam 641-010, Korea

³ Department of Applied Physics, Aalto University, P.O. Box 15100, 00076, Espoo, Finland

*e-mail: oleg@ftim.spbstu.ru

Abstract. Iron nanoparticles were prepared by chemical vapor condensation (CVC) using iron pentacarbonyl, $\text{Fe}(\text{CO})_5$, as a precursor under inert Ar and He atmospheres in a flow reactor. Subsequently, the produced nanoparticles were heat-treated at different temperatures in air. The processes of the particle morphology and phase composition changes were studied. It was found that under the continuous thermal treatment the iron nanopowders were continuously transformed from oxide-coated iron via void magnetite to large hematite nanoparticles. It was shown that low temperature heat-treatment allowed to improve magnetic properties of the oxide-coated iron nanoparticles.

1. Introduction

Iron-based nanoparticles have been extensively studied, because of their intriguing magnetic and electric properties. Various techniques have been applied for the preparation of the nanoparticles such as chemical and physical vapor condensation, spray pyrolysis, spark erosion and mechanical milling, etc. [1-5]. Especially magnetic nanoparticles possess special properties of exhibiting single-domain magnetism and can be used in magnetic tapes, ferrofluid, magnetic refrigerants, etc., because of their ultrafine size less than magnetic domain size [6]. The properties of the synthesized particles are strongly determined by preparation parameters. Also, it is well known that the properties and behaviors of nanoparticles were influenced by the chemical and phase composition, shape, and size distribution of particles [7, 8].

In this paper, we report the results of iron nanoparticle CVC synthesis from an organometallic precursor, iron pentacarbonyl, and particle oxidation behavior during the heat-treatment in the presence of air. The effects of the processing and treatment conditions on the particle size distribution and phase composition were examined.

2. Experimental

The experimental setup for the CVC synthesis of nanoparticles has been described elsewhere [9]. Briefly, the liquid precursor, $\text{Fe}(\text{CO})_5$, was heated in a bubbler, evaporated and transported by inert (argon or helium) flow in a heated tubular furnace. The tubular furnace provides a heat source for the controlled decomposition of the precursor. The product of the precursor decomposition was collected in a vacuum chamber on the surface of a rotating chiller cooled by liquid nitrogen. An iron particle passivation process was achieved by dosing

oxygen before opening the chamber to air. The loose powder was smoothly stripped off from the cold finger. The precursor decomposition temperature was maintained at 400 °C (sample 1), 750 °C (sample 2), and 1100 °C (sample 3). Thermo-gravimetric analysis (TGA) of the produced nanoparticles was conducted in an air atmosphere at the heating rate of 10 °C/min in the range of 40 – 1000 °C. The phase analysis of the samples was carried out on RIGAKU Geigerflex diffractometer with monochromatic $\text{CuK}\alpha$ radiation. The morphology and particle size distribution were determined by means of transmission electron microscopy (TEM) using JEOL JEM-2000FXII equipment. The powder for TEM investigations was ultrasonically dispersed in ethanol and dropped on a carbon coated copper grid. The number size distribution for each sample was measured from TEM images. Magnetic property measurements were carried out at room temperature using vibrating sample magnetometry VSM by saturating the sample in a field of 20 kOe.

3. Results and discussion

Fig. 1(a) presents the results of the statistical size measurements of the as-prepared particles produced and heat-treated at different temperatures. The experimental results were satisfactorily fitted with the lognormal distribution function. As can be seen from Fig. 1(a) the mean particle size increases with increasing the decomposition temperature: samples 1 (400 °C), 2 (750 °C), and 3 (1100 °C) have average particle sizes of 11.8, 19.6, and 25.0 nm, respectively. It is worth noting that the decomposition temperature increase results in wider and more asymmetrical size distributions. Experimental investigations carried out at temperatures below 400 °C revealed no particle formation.

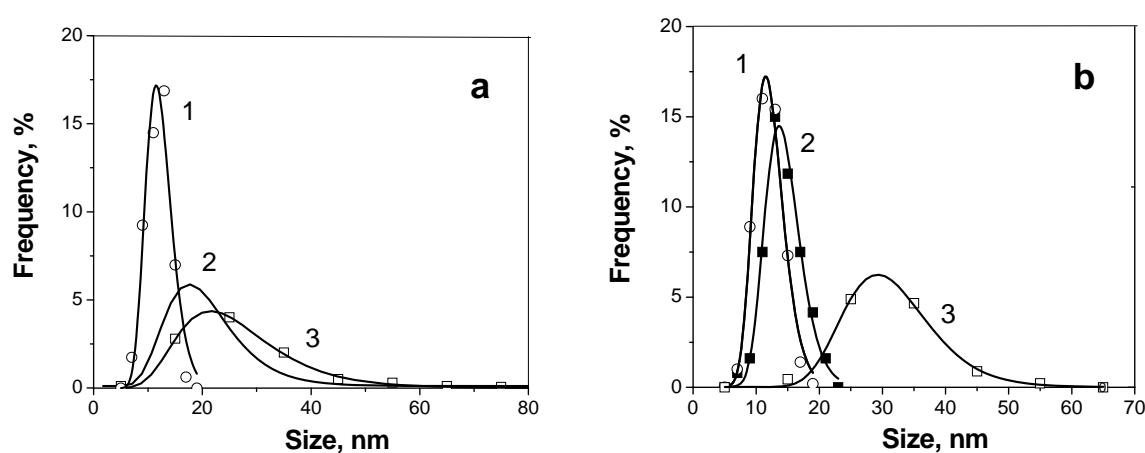


Fig. 1. Size distributions of particles prepared by CVC process using argon as a carrier gas: (a) as-prepared iron particles: decomposition temperature is 400 °C (curve 1), 750 °C (curve 2), and 1100 °C (curve 3); (b) sample 1 heated to 300 °C (curve 1), 400 °C (curve 2), and 700 °C (curve 3).

High resolution TEM observation of the as-prepared product revealed the formation of particles with a dark core and a light shell as shown in Fig. 2(a). The shells are about 3 nm thick, independently of the particles size, and consist of oxides likely formed after exposing the particles to the ambient atmosphere. However, X-ray diffraction patterns revealed only slight diffusive peaks corresponding to oxide, while the main contribution in the patterns was

obtained from BCC iron. The measured values of the lattice constant are larger than that of pure iron ($a_{\text{BCC-Fe}}=2.866 \text{ \AA}$) and increase with decreasing the particle size as shown in Fig. 2(b). This behavior of the lattice constant on the average particle size can be explained by the interaction between the metallic core and oxide shell if the growth of oxide is assumed to be epitaxial [10, 11] with a lattice misfit of about 3%. That can lead to compressive stresses induced in oxide shell and tensile stresses in metallic core, which causes increasing lattice constant in oxide-coated nanoparticles.

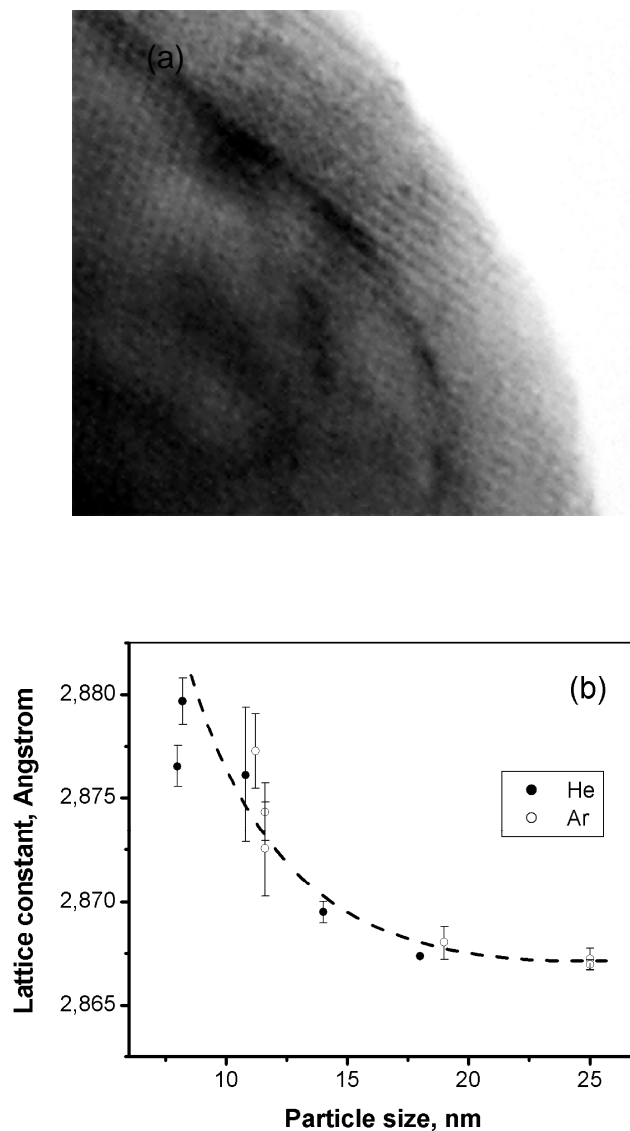


Fig. 2. High resolution TEM image of (a) metal (plane (111) BCC iron) – oxide phase interface and (b) the lattice constant of BCC iron as a function of mean particle diameter.

In order to examine the product transformation under the oxidation conditions we heated up sample 1 to different temperatures in the air atmosphere and subsequently investigated the product. Figure 1(b) and Figures 3 and 4 show the particle size distributions and TEM images of the particles treated at different conditions.

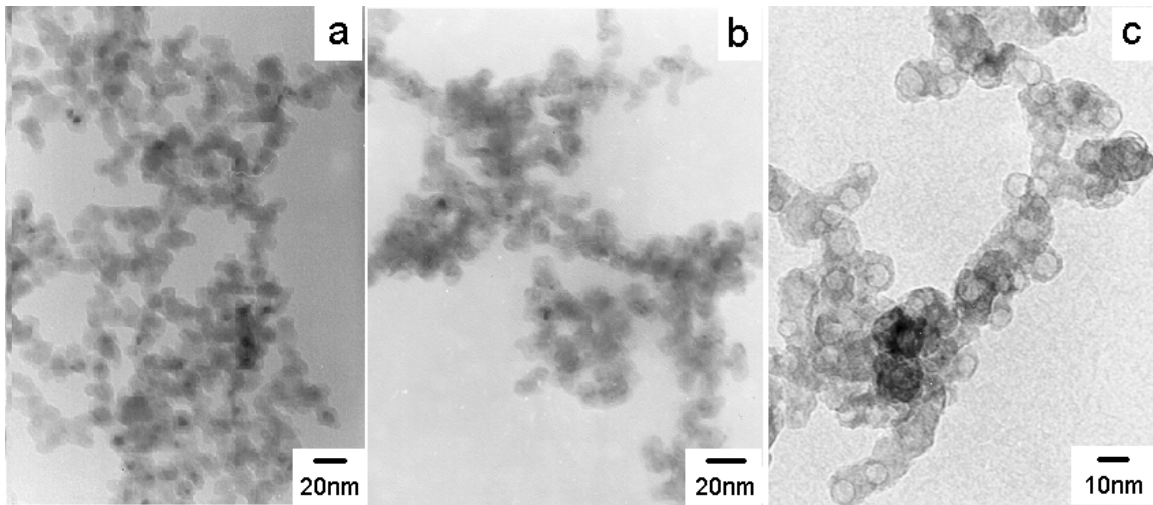


Fig. 3. TEM images of particles: (a) as-prepared; (b and c) selected images after heating to 300 °C at a rate of 10 K/min.

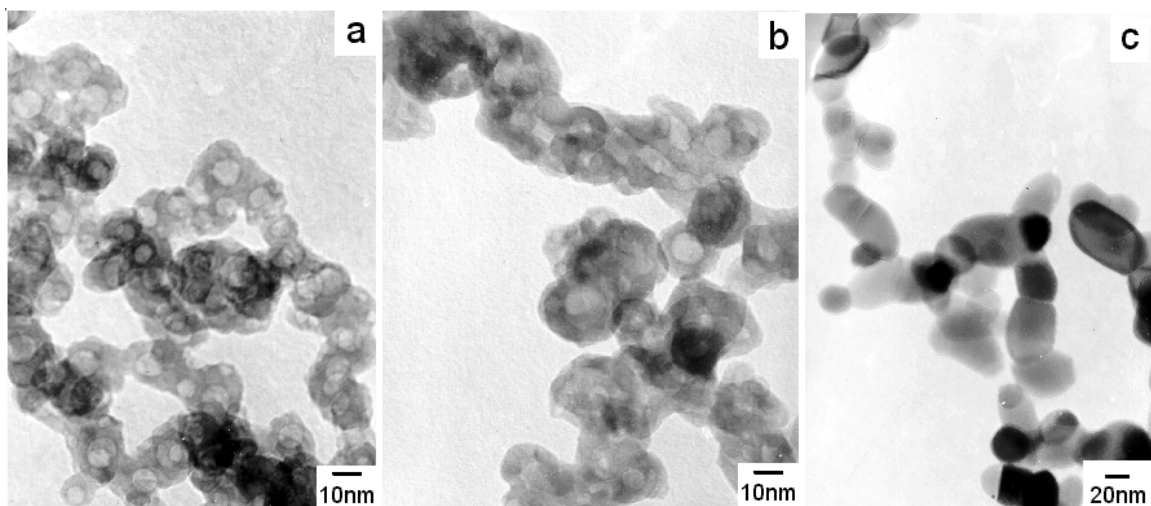


Fig. 4. TEM images of particles: heating to (a) 400 °C, (b) 500 °C, (c) 700 °C at a rate of 10 K/min.

Heating the sample to 300 °C led to a very slight increase of the particle size (within the experimental error). Higher heating temperatures resulted in more significant size increase: heating at 400 °C changes the particle sizes from 12.0 up to 14.3 nm. Also, the sample treated at 400 °C exhibits more asymmetrical size distribution. Further temperature increase increased the particle size even more significantly: up to 30.8 nm at the temperature of 700 °C.

An analysis of the experimental data including TGA curves (Fig. 5), TEM images, and X-ray diffraction results (Fig. 6) revealed that about 90 % of particles did not show significant changes in particle sizes and morphologies during the particle oxidation processes at 300 °C (Fig. 2(a,b)). However, structural changes are significant for small particles (Fig. 3(c)).

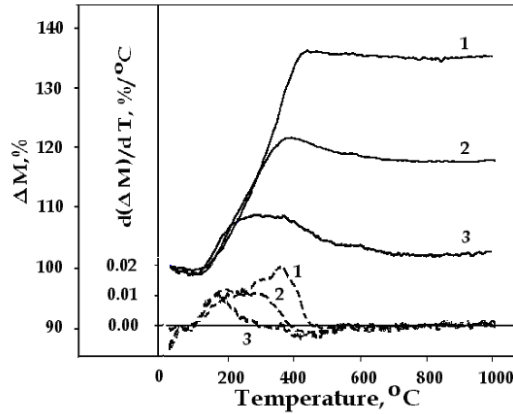


Fig. 5. Relative mass (ΔM) (solid lines) and $d(\Delta M)/dT$ (dashed lines) of iron nanoparticles versus heating temperature (T) upon heating at a rate of 10K/min. Mean particles size is (1) 25 nm, (2) 19.6 nm and (3) 11.8 nm.

Heating particles to 400 °C in the oxidation condition produced the particles consisting of light cores and dark shells as appeared in TEM images (Fig. 4a). Similar structures were observed in earlier studies, for instance, in [3, 12]. We believe that the particles consist of the internal voids and oxide shells.

That can be supported by several reasons:

- (i) mechanism of mass-thickness contrast in bright-field TEM image indicates that thicker (or higher mass) areas will appear darker contrast than thinner (lower mass) areas [12, 13];
- (ii) particle cores always have lighter contrast independently of the particle orientation (the atomic plane orientation must cause the contrast changes); and
- (iii) the assumption of the formation of internal voids can explain the significant increase in the mean particle size as can be seen in Fig. 1(b). Besides, at the heat-treatment temperature of 400°C the initial stage of the particle coalescence can be observed. That leads to the increase of the relative quantity of large particles. However, the major coalescence process begins at higher temperatures.

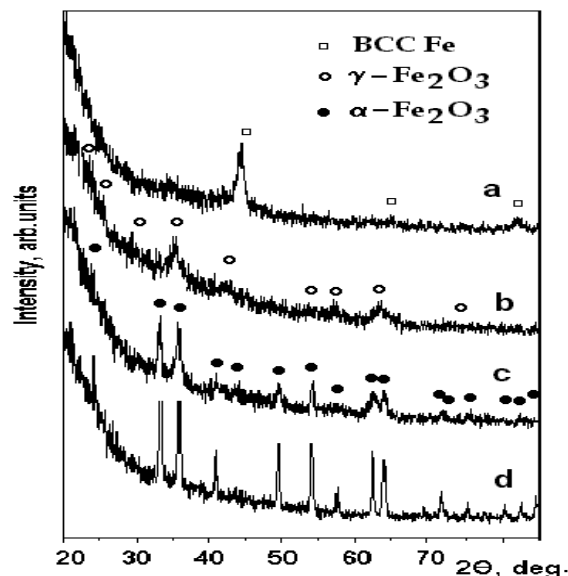


Fig. 6. X-ray diffraction pattern of (a) as-prepared nanoparticles, and same particles after heating to (b) 400 °C, (c) 500 °C, (d) 700 °C at a rate of 10 K/min.

For the powder heat-treated at 500 °C, only hematite phase was observed. However, at this condition, it was difficult to estimate the particle size from TEM images (Fig. 4(b)), since isolated particles almost completely disappeared. The particles formed a continuous structure (partially sintered) by the shells and internal voids association. Only very few individual particles could be found among the sample in TEM images. At the same temperatures (400-500°C), the substantial weight reduction (Fig. 5), especially for small particles, was observed.

Further increase of the treatment temperature to 700 °C led to the formation of hematite particles with larger sizes however without the core-shell structure (Fig. 4(c)). The size distribution of these hematite particles (for sample 1) is presented in Fig. 1(b), curve 3. As was found, the size of the new structural particles depends on initial particle size; after heating samples 1 and 2 (with the initial sizes of 11.8 and 19.6 nm) to 700 °C hematite particles were produced with sizes of 30.8 and 48.0 nm, respectively. Further heating the samples to 1000 °C resulted in insignificant particle growth.

The influence of low temperature heat-treatment on lattice constant and magnetic properties of iron nanoparticles is shown in Fig. 7. We believe that the drastic decreasing of lattice parameter of BCC phase, during low temperature heating at the temperatures higher than 250 °C, is due to the formation of defect structure in the oxide-metal phase interface by the oxide film growth, and relaxation of internal stresses [11]. Those processes lead to the increasing of saturation magnetization of nanoparticles in spite of the decreasing of iron volume fraction.

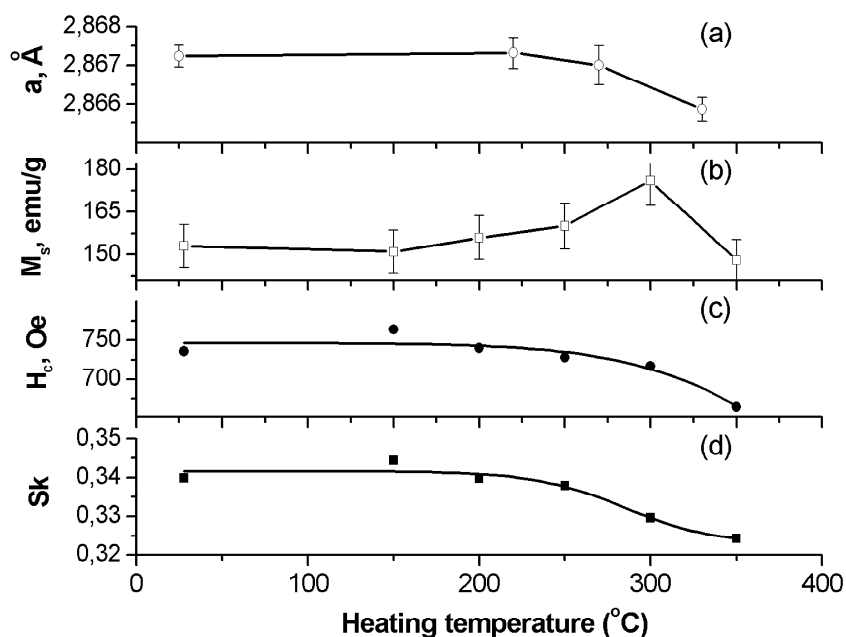


Fig. 7. Temperature dependence of (a) lattice parameter of nanoparticles, (b) saturation magnetization, (c) coercivity and (d) rectangularity of magnetic hysteresis loop.

4. Conclusions

Iron nanoparticles were prepared by chemical vapor condensation process using iron pentacarbonyl as a precursor in a flowing inert (argon or helium) atmosphere. Mean particle size was varied from 11 to 25 nm by changing the precursor decomposition temperature from 400 to 1100 °C. Increasing decomposition temperature resulted in the increase of both particle size and the broadness of the peaks and in more asymmetric particle size distributions.

An oxidation heat-treatment of the produced iron particles leads to the successive formation of oxide phases. At the temperature of about 300 °C the structure of some particles is appeared to have internal voids. Processes of the particles coagulation and maghemite-hematite transformation, starts at the temperature of about 400 °C and leads to the disappearance of the individual particles and formation of continuous (partially sintered) structures. The newly formed large hematite particles of 30-50 nm in diameter are formed at the temperature of 600 °C without significant increase in the size with the further temperature increase. The mean size of hematite particles depends on the initial size of iron particles.

Low temperature heat-treatment of iron nanoparticles revealed the drastic decrease in the lattice parameters of iron. It was revealed an increase in the saturation magnetization of nanoparticles, which can be used to improve magnetic properties of oxide-coated iron nanoparticles.

This work was supported by the Academy of Finland and by the Federal Agency for Science and Innovation.

References

- [1] I. Nobory, O. Yoshihary, K. Seiichiro, *Superfine Particle Technology* (Springler-Verlag, Heidelberg, 1988).
- [2] D. Chen, R. Hu, // *Mater. Research Bulletin* **33** (1998) 1015.
- [3] Z.L. Cui, L.F. Dong, Z.K. Zhang // *Nanostructured Mater.* **5** (1995) 829.
- [4] D. Kim, E.S. Vasilieva, A.G. Nasibulin, D.W. Lee, O.V. Tolochko, B.K. Kim // *Mater. Sci. Forum* **9** (2007) 534.
- [5] A. Moisala, A.G. Nasibulin, S.D. Shandakov, H. Jiang, E.I. Kauppinen // *Carbon* **43** (2005) 2066.
- [6] G.C. Hadjipanayis, G.A. Prinz, *Science and Technology of Nanostructured Magnetic Materials* (Plenum Press, New York, 1991).
- [7] G. Schimanke, M. Martin // *Solid State Ionic* **136-137** (2000) 1235.
- [8] L. Hu, M. Chen // *Mater. Chem. and Phys.* **43** (1996) 212
- [9] W. Chang, G. Skandan, S.C. Danforth, M. Rose, A.G. Balogh, H. Hahn, B. Kear // *Nanostructured Mater.* **6** (1995). 321.
- [10] K.K. Fung, B. Qin, X.X. Zhang // *Mater. Sci. and Eng.* **A286** (2000) 135.
- [11] C.J. Choi, O. Tolochko, B.K. Kim // *Materials Letters* **56** (2002) 289.
- [12] A.G. Nasibulin, O. Richard, E.I. Kauppinen, D.P. Brown, J.K. Jokiniemi, I.S. Altman // *Aerosol Sci. Tech.* **36** (2002), 899.
- [13] B. Fultz, J. M. Howe, *Transmission Electron Microscopy and Diffractometry of Materials* (Springer-Verlag, Heidelberg, 2001).